Magnetoresistance of Thallium in Large Magnetic Fields*

R. C. YOUNG
Institute for Atomic Research and Department of Physics, Iowa State University, Ames, Iowa
and
Cavendish Laboratory, Cambridge, England†
(Received 26 April 1967)

We have measured the transverse magnetoresistance of a *c*-axis crystal of pure thallium at liquid-helium temperatures and in magnetic fields up to 150 kG (at the National Magnet Laboratory). At 1.2°K the resistance has saturated at this field for all directions in the basal plane. The field dependence of the resistance is correctly simulated by a simple model of orbits which become coupled by magnetic breakdown. By fitting the experimental results with the predictions of the model, we are able to estimate values of the breakdown field H_0, the largest value encountered being 220 kG. The model also correctly predicts the change of resistance with mean free path between 4.2 and 1.2°K.

I. INTRODUCTION

IN large magnetic fields and at low temperatures, the magnetoresistance of a pure metal reflects the topology of the orbits described by electrons on the Fermi surface.[1] For the pure metals now available, the necessary criterion that $\omega_c\tau\gg1$, (where ω_c is the cyclotron frequency of closed orbits and τ is the relaxation time for electron scattering) for all closed orbits is readily achieved in fields of 10 kG. But in some metals, such as thallium, the energy gap Δ across one of the Brillouin-zone faces is quite small and some electrons are able to tunnel through the energy gap, this process being known as magnetic breakdown.[2] An electron now has a probability $P[=\exp(-H_0/H)]$ of tunneling to another orbit on the Fermi surface and the resultant change of topology will be reflected in the magnetoresistance.

For nearly free electrons with an energy gap Δ, and **H** in the z direction

$$H_0=\pi\Delta^2/4\hbar e v_x v_y, \tag{1}$$

where v_x and V_y are components, respectively parallel and perpendicular to the zone boundary, of the "free-electron velocity" at the zone boundary, i.e., the velocity which the electron would have in the absence of the energy gap.[3] In the special case where $v_x=v_y$ and there is no component of v parallel to the field, Eq. (1) for H_0 reduces to

$$H_0=\pi\Delta^2 m/4\hbar e E_F, \tag{2}$$

where m is the electronic mass and E_F is the Fermi energy.

In the presence of magnetic breakdown, there is considerable variation of the resistance with field even at fields well above H_0, and a field of at least this magnitude is required. Our previous studies of the magnetoresistance of thallium[4] (hereafter referred to as I) were mainly in fields below 55 kG, and it was clear from them that some values of H_0 on the Fermi surface of thallium were considerably larger than this. In the present work we report measurements of the magnetoresistance up to 150 kG which show that the effects of magnetic breakdown are becoming complete at this magnitude of field for all field directions in the basal plane of thallium. We calculate the detailed behavior of a simple model to simulate the effect of magnetic breakdown on the magnetoresistance and by fitting the experimental results to the calculated behavior we are able to estimate values of H_0 for thallium, the largest being 220 kG.

In Sec. II we briefly describe the Fermi surface of thallium and calculate the magnetoresistance of a special model of coupled orbits. In Sec. III we mention the experimental technique and present the experimental results which will then be analyzed in the light of our calculations of Sec. II.

II. THEORY

A. Fermi Surface of Thallium

Thallium is a hexagonal close-packed metal with a hexagonal reciprocal lattice. In the absence of spin-orbit coupling, the energy gap across the (0001) face (AHL in Fig. 1) between the third and fourth Brillouin zones would be zero. This degeneracy is lifted by the spin-orbit coupling except along the lines AL, the energy gap varying from zero on a line AL to a maximum value at a corner H.

The Fermi surface of thallium has been studied experimentally by magnetoresistance,[4–6] the de Haas–van

* Work performed in the Ames Laboratory of the U. S. Atomic Energy Commission. Contribution No. 2013.
† Present address.
[1] For a review of this topic, see E. R. Fawcett, *Advances in Physics* (Francis and Taylor, Ltd., London, 1964), Vol. 13, p. 139.
[2] M. H. Cohen and L. M. Falicov, Phys. Rev. Letters **7**, 231 (1961).
[3] E. I. Blount, Phys. Rev. **126**, 1636 (1962).
[4] J. C. Milliken and R. C. Young, Phys. Rev. **148**, 558 (1966), hereafter referred to as I.
[5] A. R. Mackintosh, L. E. Spanel, and R. C. Young, Phys. Rev. Letters **10**, 434 (1963).
[6] N. E. Alekseevski and Yu. P. Gaidukov, Zh. Eksperim. i Teor. Fiz. **43**, 2097 (1962) [English transl.: Soviet Phys.—JETP **16**, 1484 (1963)].

Alphen effect,[7] and the magnetoacoustic effect.[8,9] All of these measurements show the Fermi surface to be in good agreement with that of the relativistic orthogonalized plane-wave calculation by Soven[10,11] (the ROPW model). They indicate that magnetic breakdown occurs across the zone face AHL between the third and fourth Brillouin zones.

Figure 1(a) is a drawing of the Fermi surface of thallium. This is in fact the nearly-free-electron model modified to be topologically similar to the ROPW model, but this will be adequate for our purposes. Soven[11] suggested that the arms of the fourth-zone surface which extend in the [0001] direction are pinched off before the top of the zone is reached, which was confirmed in I. There are other fragments of the Fermi surface in the fifth and sixth zones.

The important characteristic of the ROPW model from the point of view of magnetoresistance is that open orbits are able to propagate in directions parallel to the (0001) plane if they are able to tunnel through the face AHL between the third and fourth zones. A typical open orbit is shown in Fig. 1(a). When breakdown is complete, the surface becomes a pair of open sheets in the (0001) plane, and open orbits in directions parallel to this plane will exist for all field directions (except those exactly parallel to the c axis). For a c-axis specimen with the magnetic field in the basal plane, breakdown changes the magnetoresistance from the H^2 behavior of a compensated metal to the saturation expected for open orbits perpendicular (in k space) to the current. In the next section we discuss the expected behavior in detail.

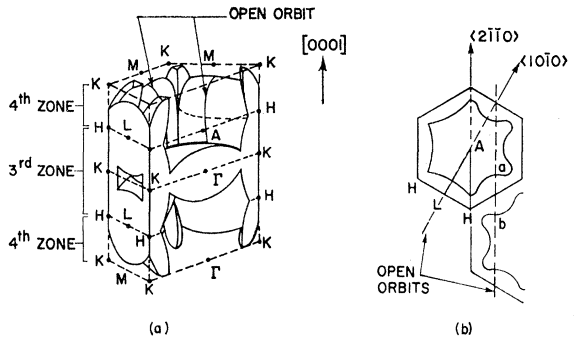

FIG. 1. (a) Third and fourth zones of the free-electron model for thallium. The typical open orbit is able to propagate parallel to a direction in the basal plane if breakdown allows it to cross the zone face AHL between the third and fourth zones. (b) A (0001) section of the fourth-zone surface on the plane AHL showing the free-electron model section on the left and the ROPW model section on the right. The optimum orbits in the [10$\bar{1}$0] and [2$\bar{1}\bar{1}$0] directions are indicated.

[7] M. G. Priestley, Phys. Rev. **148**, 580 (1966).
[8] J. A. Rayne, Phys. Rev. **131**, 653 (1963).
[9] Y. Eckstein, J. B. Ketterson, and M. G. Priestley, Phys. Rev. **148**, 586 (1966).
[10] P. Soven, Phys. Rev. **137**, A1706 (1965).
[11] P. Soven, Phys. Rev. **137**, A1717 (1965).

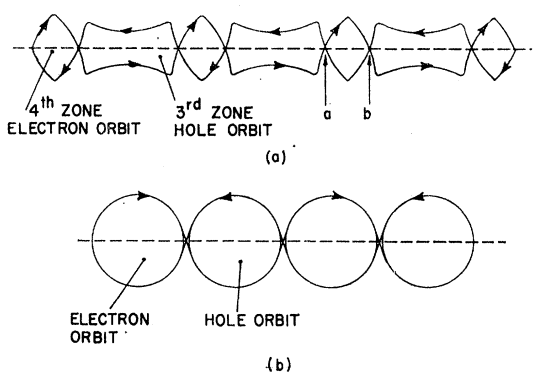

FIG. 2. (a) The network of third-zone hole orbits and fourth-zone electron orbits which become coupled by magnetic breakdown to form an open orbit parallel to [10$\bar{1}$0]; (b) a simple model of coupled orbits formed from circular electron and hole orbits.

B. Expected Magnetoresistance of Thallium

In this section we set out to calculate the field dependence we expect in the resistance of a [0001] specimen when the magnetic field is in the (0001) plane. We first examine some of the systems of coupled orbits produced by breakdown. Figure 2(a) shows the open orbit in the [10$\bar{1}$0] direction, which passes through the symmetry point A of the plane AHL. It opens by coupling hole orbits on the third-zone surface with electron orbits on the fourth-zone surface. The example we have shown runs along the line AL and so actually encounters no energy gap. Neighboring orbits will be very similar, but they will encounter a progressively larger energy gap as they pass nearer to the point H of largest energy gap.

The coupled-orbit system in the [2$\bar{1}\bar{1}$0] direction, which crosses the lowest energy gap while still having equal gaps at "a" and "b" is similar to Fig. 2(a), but the value of the gap is not zero as it was for [10$\bar{1}$0]. This orbit passes through point L in the AHL plane. Neighboring orbits will have a larger gap at a and a smaller gap at b (or vice versa). For other rational directions, and for nonrational directions in the basal plane, the open orbits will still be formed by coupling third-zone hole orbits and fourth-zone electron orbits, but the loss of symmetry means that the orbit will repeat itself only over a very large number of reciprocal lattice vectors, in contrast to the cases of Fig. 2(a) which are periodic in the zone separation, while the value of the energy gap will not be the same at each junction.

On the actual Fermi surface there will be a number of coupled orbits for different values of k_H, and these will break down at different fields. Some "optimum orbits" (this concept is also used in I) will be the first to open, and as the field is increased orbits for nearby k_H values will open until finally all orbits are open. Clearly, the resistance will be dominated by the open orbits long before all orbits are actually open, and so we will assume that a suitable model for simulating the resistance can be made if a certain fraction of the electrons lie on

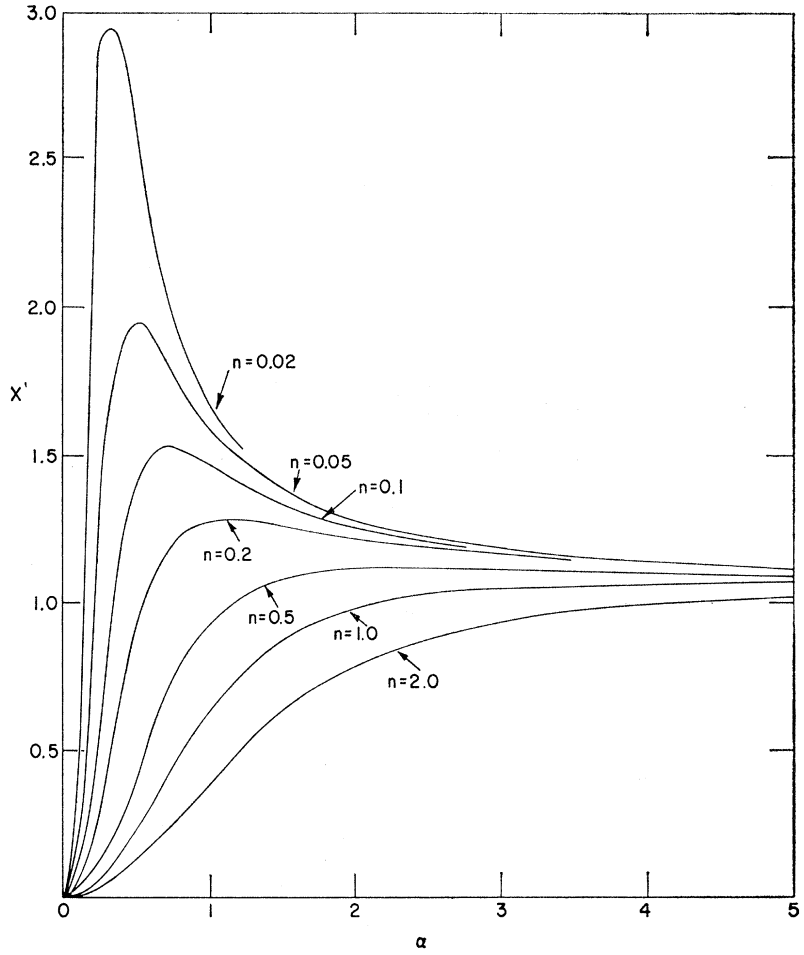

FIG. 3. Curves of X versus α for various values of n [from Eq. (5)].

orbits which are coupled by breakdown while the rest do not.

Away from the main symmetry directions, the systems of coupled orbits are clearly too complicated for their properties to be calculated analytically. We will therefore consider a simple model of circular electron and hole orbits coupled by breakdown with probability $P(Q=1-P)$. We will then use the behavior of this model as a guide in discussing the experimental results, even for field directions for which the orbits are more complicated. Figure 2(b) shows this coupled-orbit system. At low fields ($H<H_0$), it consists of an equal number of electron and hole orbits to simulate the compensation of thallium in the absence of breakdown. At high fields ($H>H_0$), the orbits are linked to form an open orbit.

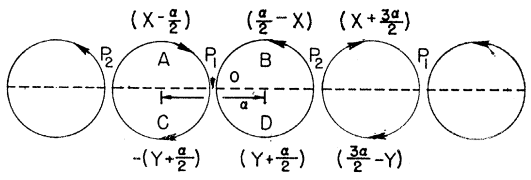

FIG. 4. A model of coupled circular electron and hole orbits with different breakdown probabilities P_1 and P_2 at alternate coupling points.

We will, of course, first calculate the components of the conductivity tensor and obtain the resistivity from it by inversion. We will assume that the magnetic field is in the z direction and that the coupled-orbit system is in the x direction in real space. For our system of orbits we may readily write $\sigma_{xz}=\sigma_{zx}=\sigma_{yz}=\sigma_{zy}=0$ and $\sigma_{zz}=$ const. We will in fact assume that these simplifications apply to the complete Fermi surface. The remaining components are calculated for the network of Fig. 2(b) using the effective-path method developed by Pippard.[12,13] This calculation is carried out in Appendix A and shows that the field and relaxation time (τ) dependence of these conductivity components is given, to lowest order in H^{-1} by

$$\begin{aligned}&\sigma_{yy}=A/\omega^2\tau,\\&\sigma_{xy}=-\sigma_{yx}=0\ [\text{actually of order } H^{-2}],\\&\sigma_{xx}=B(P+Q/\omega\tau)/H(2Q+\pi/\omega\tau),\end{aligned}\qquad(3)$$

[12] A. B. Pippard, Proc. Roy. Soc. (London) **A282**, 464 (1964).
[13] A. B. Pippard, Proc. Roy. Soc. (London) **A287**, 165 (1965).

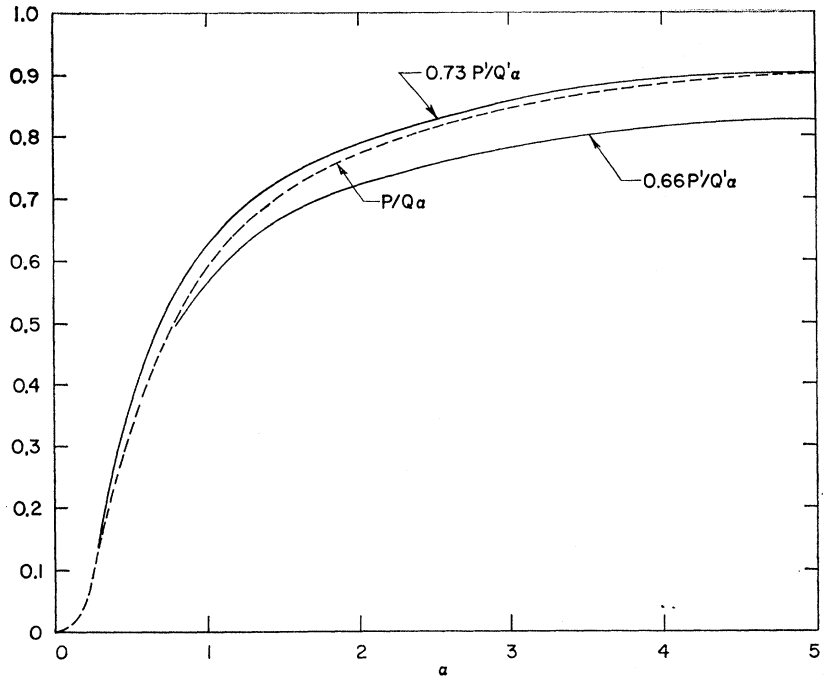

FIG. 5. Curves of $P/Q\alpha$, 0.73 $P'/Q'\alpha$, and 0.66 $P'/Q'\alpha$ versus α.

where A and B are constants which will depend on the number and velocity of the electrons on the chain of coupled orbits. If $Q\gg\pi/2\omega\tau$, we may simplify σ_{xx} to give

$$\sigma_{xx}=BP/2QH+B/2H\omega\tau. \tag{4}$$

Since $Q=H_0/H$ at high fields, the condition $Q\gg\pi/2\omega\tau$ may be written $\omega_0\tau\gg\pi/2$, where $\omega_0=eH_0/m$. Equation (4) is thus valid for all fields, independent of H, as long as H_0 is sufficiently large and $\omega\tau\gg1$.

We must take account of other parts of the Fermi surface not on the chain of coupled orbits, and this will add terms proportional to $1/\omega^2\tau$, to σ_{xx}, and σ_{yy}. Compensation ensures that σ_{xy} is still zero. It should be noted that for the coupled-orbit system of Fig. 2(a), σ_{xy} is not in fact zero because there is not an equal number of electrons and holes on this system. However, as discussed in Appendix B, σ_{xy} for a linear chain of coupled orbits is not altered by breakdown, so that if $\sigma_{xy}=0$ for the whole Fermi surface before breakdown, $\sigma_{xy}=0$ after breakdown. The complete conductivity tensor is thus

$$\sigma=\begin{bmatrix}\sigma_{xx} & 0 & 0\\ 0 & C/\omega^2\tau & 0\\ 0 & 0 & \text{const}\end{bmatrix},$$

where $\sigma_{xx}=BP/2QH+K/\omega^2\tau$, C and K being constants. This is readily inverted to give $\rho_{xx}=1/\sigma_{xx}$.

Examining the field dependence of ρ_{xx} at low and high fields, we find that when $H\ll H_0$, $\rho_{xx}\approx\omega^2\tau$ while at high fields, where $Q\approx H_0/H$ and $P\approx1$, we find that $\rho_{xx}\approx[2H_0+H\pi/\omega\tau]/B$. Thus at low fields the resistance follows an H^2 dependence as expected for a compensated metal with no open orbits, while at high fields it saturates as expected for open orbits in the direction in reciprocal space at right angles to the current. In the absence of breakdown, the resistance due to an open orbit is proportional to $1/\tau$, and for our example with breakdown we could follow Falicov and Sievert[14] in writing the resistance as proportional to $1/\tau_1$, where

$$1/\tau_1=1/\tau+2Q\omega\approx1/\tau+2H_0e/m\pi$$
$$=1/\tau+2\omega_0/\pi.$$

Writing $\alpha=H/H_0$ and $Y=B/2H_0$, we exhibit the resistance as a function of field and H_0 in the form of universal curves of X versus α for various values of a parameter n, where

$$1/X=1/Y\rho_{xx}=[P/Q\alpha+n/\alpha^2], \tag{5}$$

and $n=(2K/H_0B\tau)(m/e)^2$. These curves are shown in Fig. 3. It is of interest to note that a peak in resistance versus field occurs for small values of n, always at $\alpha\leq1$, while for large values of n no peak occurs but the resistance increases monotonically.

For a network as simple as that of Fig. 2(b), the values of H_0 may be found from an experimental curve of ρ versus H merely by selecting that curve from the family which gives the best fit to the shape, H_0 being the scaling factor between H and α. This means that H_0 can be found from the shape without knowing the relative number of electrons on the open orbit or τ. In thallium, τ may be varied by an order of magnitude over the temperature range 4.2 to 1°K, and this will

[14] L. M. Falicov and P. R. Sievert, Phys. Rev. 138, A22 (1965).

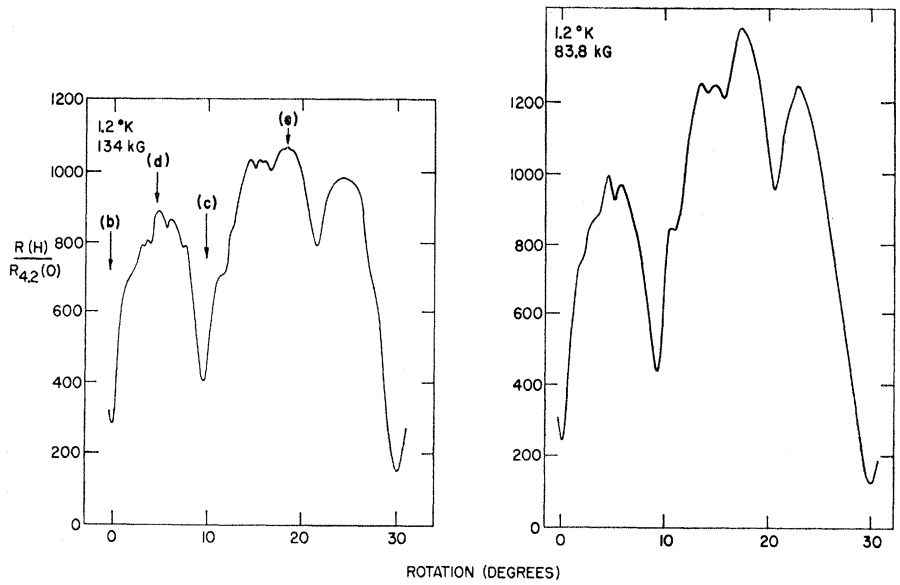

FIG. 6. Experimental plots of resistance versus angle of the magnetic field in the basal plane, measured from $[10\bar{1}0]$, at 1.2°K and for fields of 83.8 and 134 kG.

change the appropriate value of n and, hence, the shape of ρ versus H.

When the field is in an arbitrary direction in the basal plane, it is not obvious that the results of our simple model can be applied. Even a typical optimum orbit will break through at various values of P for its various intersections with the plane AHL. We will show later that the experimental results for arbitrary directions are in fact well simulated by Eq. (5), and we must ask what the H_0 values obtained from curve fitting actually refer to. It might be expected that the resistance due to a particular open orbit would reflect the largest H_0 value encountered by that orbit. We will consider a simple example to show that this is a reasonable conclusion.

Let us consider the network shown in Fig. 4. This still consists of identical circular electron and hole orbits, but the breakdown probability will be given the values P_1 and P_2 at alternate coupling points along the network. We will again use the effective-path method[13] to calculate the conductivity. We have already shown that as long as $\omega_0\tau \gg \frac{1}{2}\pi$, the only effect of introducing a finite relaxation time is to add a term proportional to $1/\omega^2\tau$ to the conductivity calculated for $\tau \to \infty$. We will therefore calculate the conductivity in this limit.

The network now has less symmetry than that of Fig. 2(b) and the center of symmetry we will use is point 0. X and Y are the mean terminal points of the arcs, referred to their own centers, while the values of mean terminal points such as $(X-\frac{1}{2}a)$ are referred to the center 0 and so make use of the symmetry about this point. The equations linking X and Y are

$$\begin{aligned}(X-\tfrac{1}{2}a)&=P_1(Y+\tfrac{1}{2}a)-Q_1(Y+\tfrac{1}{2}a),\\ (Y+\tfrac{1}{2}a)&=P_2(X+\tfrac{3}{2}a)+Q_2(\tfrac{1}{2}a-X),\end{aligned} \tag{6}$$

and these may be solved to give

$$X=\frac{a[2P_1P_2+P_1-P_2]}{2[P_1+P_2-4P_1P_2]},\quad Y=\frac{a[2P_1P_2+P_2-P_1]}{2[P_1+P_2]-4P_1P_2}. \tag{7}$$

The conductivity due to the network may now be written

$$\begin{aligned}\sigma_{xx}&=B[X+Y]\\ &=2BaP_1P_2/[(P_1+P_2)-2P_1P_2]\\ &=BaP'/Q'+K/\omega^2\tau,\end{aligned} \tag{8}$$

where $P'=2P_1P_2/(P_1+P_2)$, i.e., $2/P'=1/P_1+1/P_2$ and $Q'=1-P'$. This is exactly the same form as Eq. (5) if we consider a P' which is the harmonic mean of P_1 and P_2, where $P_1=\exp(-H_1/H)$, $P_2=\exp(-H_2/H)$. At fields $H \gg H_1, H_2$ we note that $\rho_{xx} \approx \frac{1}{2}[H_1+H_2]$, and thus the value of the resistivity at very high fields is proportional to the mean of the two breakdown fields encountered on the coupled-orbit system.

When H is of the same order as H_1 or H_2, the form of P suggests that the shape of the curve of ρ versus H will be dominated by the largest value of H_0 (say H_1). We illustrate this by a numerical example for $H_1=2H_2$. In Fig. 5 we show a curve of $P/Q\alpha$ versus α. This is to be compared to the curves for 0.66 $P'/Q'\alpha$ and 0.73 $P'/Q'\alpha$, where $\alpha=H_1/H$. It can be seen that although neither curve fits over all the range shown, both are quite similar in shape. In particular, it can be seen that it is possible to get a good agreement over a limited range of α merely by varying the scaling factor. Since the shape of curves for resistance versus α depend only on the shape of $P/Q\alpha$ versus α, any scaling factor being taken up by varying n, the $P'/Q'\alpha$ curve can be made to simulate $P/Q\alpha$ over that range of α where an experi-

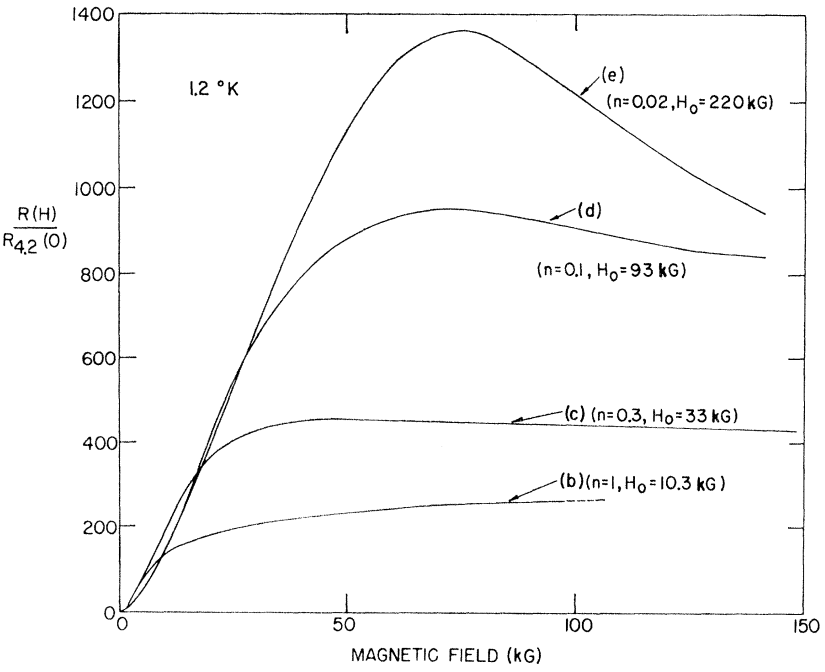

FIG. 7. Experimental plots of resistance versus field at 1.2°K for several field directions in the basal plane, the indices (b)–(e) referring to directions marked in Fig. 6. For each plot the values of n and H_0 are marked which give the best fit to the curves of Fig. 3.

mental curve is being fitted, giving an error in the estimated value of H_1 of only a few percent. Thus, in this simple example, the value of H_0 to be obtained by fitting an experimental curve to Eq. (5) will be close to H_1, the largest of the two values encountered by the open orbit. We will assume that we can apply this result to more complicated cases.

To summarize, the calculations of this section suggest that the shape of an experimental curve of resistance versus H may be fitted to Eq. (5) to give a value of H_0, and this will be a good approximation to the largest value of H_0 encountered by the open orbit. The value of n will depend on τ and H_0 as well as on the fraction of the carriers which are on the coupled-orbit system. The value of the resistance at very high fields will be proportional to the average value of H_0 along the orbit rather than the maximum value.

III. EXPERIMENTAL RESULTS AND DISCUSSION

A. Experimental Technique

The experimental technique is the same as that described in I. The measurements were carried out both at 4.2 and 1.2°K in a conventional copper solenoid at the National Magnet Laboratory, the maximum field reached being 150 kG.

The specimen was prepared as described in I from pure thallium supplied by Cominco, Inc. The resistance ratio between the room temperature and 4.2°K was 11 000, and this improved to approximately 100 000 as the temperature was lowered to 1.2°K.[15] At this low temperature the specimen was, of course, superconducting, and the resistance had to be determined by extrapolating measurements at fields sufficiently large to destroy the superconductivity.

[15] I am grateful to R. C. Barklie for carrying out this measurement.

B. Experimental Results and Comparison with the Calculation of Sec. IIC

The experimental results for a specimen oriented parallel to the c axis are shown in Figs. 6–9. In all cases we show the resistance divided by $R_{4,2}(0)$, the resistance at 4.2°K and in zero field. The graphs thus reflect the actual resistance of the specimen rather than the conventional $\rho(H)/\rho(0)$. The graphs of resistance versus angle at constant field are for the magnetic field in the basal plane, so that only 30° of angle is required, 0° being when **H** is parallel to $[10\bar{1}0]$ and 30° when **H** is parallel to $[2\bar{1}\bar{1}0]$. Field sweeps were taken at the selected field directions marked as (a)–(e) on the rotation graphs.

We will first concentrate the discussion on the field sweeps because these are readily compared to the calculations of Sec. II. The set of experimental curves

TABLE I. Values of H_0, n, nH_0, R_∞, and (R_∞/nH_0) for the plots of resistance versus field at 1.2°K of Fig. 6.

Angle of field from $[10\bar{1}0]$	H_0 (kG)	n	nH_0	R_∞[a]	R_∞/nH_0
0° (b)	10.3	1	10.2	280	274
9.5° (c)	33	0.3	9.9	410	415
5° (d)	93	0.1	9.3	680	730
18° (e)	220	0.02	4.4	518	1180

[a] $R(H)/R_{4.2}(0)$ as $H \to \infty$, the extrapolation being made using Eq. (5).

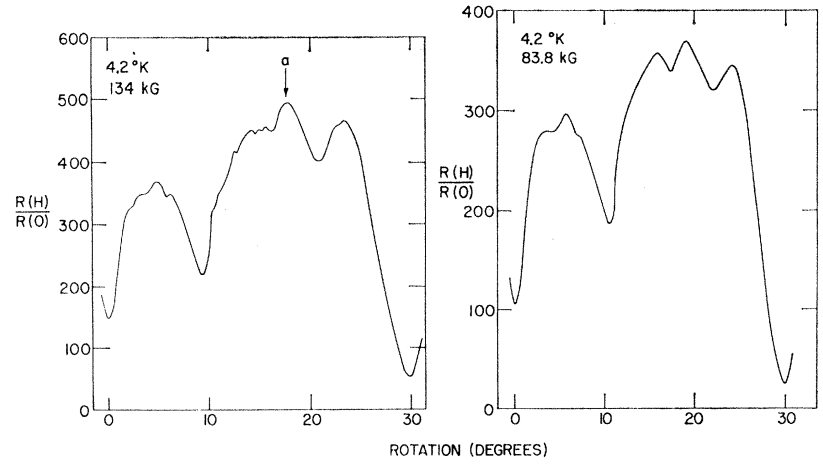

FIG. 8. Experimental plots of resistance versus angle (defined as in Fig. 6) at 4.2°K.

of Fig. 7, taken at 1.2°K, are clearly similar to some of the curves of Fig. 3, and we have marked on them the values of H_0 and n which give the best simulation of each experimental curve. We will consider the H_0 values later. It will be noticed that the curves of larger H_0 are fitted by the smaller n values. Since $n=(2/H_0 f\tau)\times(m/e)^2$, nH_0 will depend, at constant τ, on $f(=B/K)$, a number proportional to the ratio of the number of carriers on the coupled-orbit system to the total number of carriers. The values of nH_0 are displayed in Table I, and it can be seen that f is thus of about the same value for curves (b), (c), and (d) and approximately twice as large for (e).

A dramatic test of our calculation is provided by comparing the results at 4.2 and 1.2°K since τ changes by approximately a factor of 10 between these temperatures. Thus, since $n=0.02$ is appropriate for curve (e) at 1.2°K, $n=0.2$ should be correct for the same field direction at 4.2°K (H_0 remains the same). At 150 kG, α only reaches a value of 0.57 for this direction. The field sweep for direction (e) at 4.2°K is shown in Fig. 9 where it is labeled (a). It reproduces well the shape of Fig. 3 for the curve $n=0.2$, and not only is the shape correct but in fact the magnitude agrees well, the value of R at 150 kG from Fig. 9 being 500, compared to the value of 515 predicted from our theory and our results at 1.2°K.

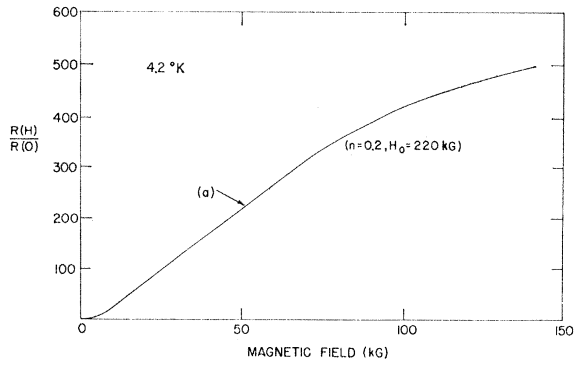

FIG. 9. Experimental plot of resistance versus field at 4.2°K for direction (a) of Fig. 8 [this is the same direction as (e) of Figs. 6 and 7].

The anisotropy curves of Figs. 6 and 8 are not very susceptible to interpretation since the limit $H\gg H_0$ is clearly not reached by 150 kG for all directions. A close examination of these curves, and those of I at lower fields, shows that the various maxima and minima occur at angles which depend on the field and temperature. This is not surprising when it is realized that the resistance at different angles is accounted for by different values of H_0 and n, but it means that little can be done with these curves except to compare them with an *ab initio* calculation if one were available. It should be noted, however, that the anisotropy is reduced at higher fields and that at 150 kG and 1.2°K there is clearly much less anisotropy in the resistance than in the values of H_0. This is in line with our conclusion of Sec. II that the high-field resistance should reflect the average value of H_0, not the maximum value. We examine this in detail for the directions of (b)–(e). In Table I we show $R_\infty[=R(H\to\infty)/R(0)]$ obtained by extrapolating the experimental curves of R versus H using Eq. (5). Notice that R_∞ at (e) is less than R_∞ at (d) even though H_0 is much larger for (e) than for (d). This occurs because R_∞ reflects f, the fraction of carriers on the coupled orbit system, as well as $\bar{H}_0$. In fact, $\bar{H}_0\sim fR_\infty$, and so is proportional to R_∞/nH_0. This is also shown in Table I, and it can be seen that the values of R_∞/nH_0 now reflect the fitted values of H_0 but with the reduced anisotropy to be expected for $\bar{H}_0$.

C. Comparison with the Fermi Surface of Thallium

So far we have analyzed the experimental results in terms of the model of Sec. IIB, without much regard for the fine details of the Fermi surface of thallium. The model in fact simulates the results well and appears to be internally consistent. There still remains the problem of relating our values of H_0 to actual points of inter-

section of the Fermi surface with the plane AHL. We recall that the electrons travel in planes perpendicular to the plane AHL between the third and fourth zones and that an open orbit can exist if breakdown allows an electron to tunnel through the energy gap each time it intersects the plane AHL. The energy gap varies from zero on the line AL to a maximum on the line AH.

In I we showed that Eq. (2) becomes $H_0=\pi\Delta^2 m/4\hbar eE_F \sin\varphi \sin 2\eta$, where η is the angle between the "free-electron velocity vector" and the plane AHL, while φ is the angle between $\mathbf{H}$ (which is parallel to the plane AHL) and the component of velocity in this plane. The angle φ depends on the actual field direction while all the other factors depend only on the point where the electron tunnels. Therefore, we will rewrite Eq. (2) as $H_0=H_0' \sin\varphi$. Thus, H_0' is a local property of the Fermi surface.

H_0' is a complicated function of the Fermi surface and Soven does not give sufficient detail for it to be evaluated for the ROPW model. We showed in I that the term $1/\sin 2\eta$ could vary it by a factor of 2 for different sections of the model and that this might cause the maximum value of H_0 to occur at a point different from the maximum value of the energy gap Δ. In view of this, it can hardly be surprising that we are unable to relate all of our experimental H_0 values to the Fermi surface.

The four directions (b)–(e), for which we measured the field dependence, were chosen because they were at principal maxima and minima of the curve of resistance versus angle at 134 kG and 1.2°K. (b) is the only one which is parallel to a direction of high symmetry, and its value of $H_0=10.3$ kG can readily be related to the Fermi surface. The optimum orbit for (b) is the open orbit marked for the direction $[2\bar{1}\bar{1}0]$ in Fig. 1(b). It breaks through at the same value of H_0 at each intersection with the plane AHL, so that $H_0=10.3$ kG at this point. The angle φ is approximately 90°, so that H_0' at this point is also 10.3 kG.

Since the directions (c)–(e) are not low-order rational directions, no such simple analysis is possible and we will not attempt to relate their H_0 values to specific points on the Fermi surface. We can, however, make some useful comments. In the limit of infinite mean free path, an open orbit parallel to an irrational direction in the basal plane will eventually pass through all points of intersection of the Fermi surface with the plane AHL. This would imply that the open orbits for (c)–(e) should each pass through the point of maximum H_0' and that the H_0 values would reflect this. The large range of H_0 from 33 to 220 kG clearly suggests that this is improbable. However, breakdown causes the electron to have a definite probability of leaving the open orbit at each junction, and this situation is described by the effective relaxation time τ_1 which we previously saw was of the order of $1/\omega_0$. This implies that, at normal fields, the electron stays on the open orbit for only a few lattice spacings.

TABLE II. Values of $\bar{H}_0$ and X/a for the plots of resistance versus field of Fig. 6.

Index of plot	H_0(kG)	(R_∞/nH_0)	$\bar{H}_0$(kG)	X/a at 150 kG
(b)	10.3	274	10.3	7.2
(c)	33	415	15.6	4.8
(d)	93	738	27.8	2.7
(e)	220	1180	44.4	1.7

We can get a detailed estimate of this number of lattice spacings from the effective path X since $X/a=P/2Q=H_0/2H$ when $H\gg H_0$. For the case when H_0 is not the same at all points along the orbit, we assume that $X/a=H/2\bar{H}_0$. We saw that the values of R_∞/nH_0 in Table I were proportional to $\bar{H}_0$. Since H_0 for direction (b) is the same at all breakdown points, we know that for (b) $\bar{H}_0=H_0=10.3$ kG. This allows us to estimate the values of $\bar{H}_0$ for (c)–(e), and these are shown in Table II. From these values of $\bar{H}_0$, the number of lattice spacings traversed by the electron at 150 kG, X/a, is also shown in Table II. In each case it is small, less than 10.

This helps to explain two features of the experimental results. First, the H_0 will reflect the largest value of H_0 encountered over a few lattice spacings rather than the largest H_0 along an open orbit of infinite length. These experimental H_0's thus need no longer be the largest value of H_0 on the surface, and so the wide variation we have actually found is allowed. Along an irrational direction there will be some places where the electron is able to break through at each of several consecutive junctions, while at other places it will not be able to do so. This leads to the second point, that we used a model where only some fraction f of the electrons was on the open orbit. This is unjustified on the actual Fermi surface, since at the highest fields all electrons should be on open orbits except for the minute number in zones five and six. However, we can now see that f may be less than unity since the electrons which are able to break through at several consecutive junctions will appear to be on open orbits, while those which cannot will appear to be on closed orbits.

D. Summary

In this work we have studied the high-field magnetoresistance of a c-axis crystal of thallium as a means of obtaining detailed information about the effect of magnetic breakdown on the Fermi surface of thallium. By analysis of a simple model of coupled circular electron and hole orbits we were able to obtain a family of curves for the resistance versus field as a function of H_0 and one other parameter. We were able to fit the experimental results to these curves even for directions where the real coupled-orbit system was clearly more complex. We thus obtained values of H_0 for several different field directions.

By considering a slightly more complicated model of

coupled orbits, we were led to the conclusion that these H_0 values would be the largest at which an electron on a particular orbit broke through, while the extrapolated values of the resistance at very high fields would be proportional to the average value of H_0. The experimental results reflect this. The very large change of τ between 4.2 and 1.2°K made a substantial difference in the form of the plots of resistance versus field at these temperatures, which was correctly explained by our analysis.

Except in one case of high symmetry it was not possible to allocate the values of H_0, which ranged up to 220 kG, to specific points of breakdown on the ROPW model while the model is not detailed enough to predict these values. We did show that for the field away from directions of high symmetry an electron travels on an open orbit for only a few lattice spacings in the fields we used.

ACKNOWLEDGMENTS

We are grateful to the National Magnet Laboratory for the use of its facilities and to the Science Research Council of Great Britain for support during the preparation of this paper.

APPENDIX A

In this Appendix we will derive expression (3), the expression for the conductivity of the network of coupled circular orbits of Fig. 2(b). This real space network is shown again in Fig. 10(a). The magnetic field is in the z direction while the open direction of the network is the x direction. We follow Pippard[12] in assuming that electrons are "created" at the point ϕ_0 on the orbit at a rate proportional to $E\sin\phi_0 d\phi_0$, where E, the electric field, is in the x direction. These electrons

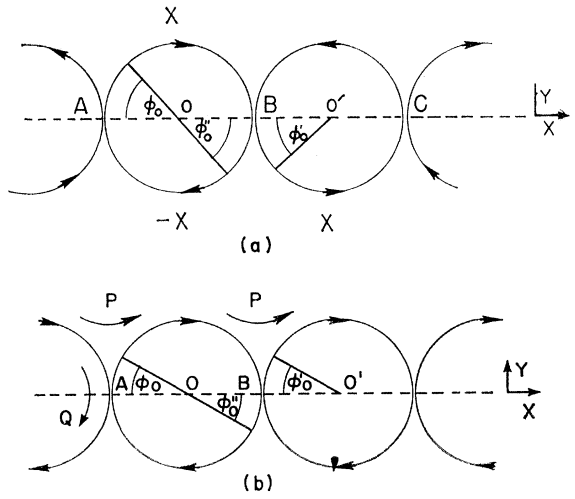

FIG. 10. (a) Model of coupled circular electron and hole-orbits; (b) model of coupled circular electron orbits.

then travel on the network under the influence of the Lorentz force until scattered, the fraction which reaches ϕ being written $f(\phi_0,\phi)$. f will reflect scattering and also the switching allowed by magnetic breakdown.

We follow Pippard in writing the effective path in the x direction for the arc AB as

$$X=\frac{1}{2}\int_0^{\pi}\sin\phi_0 d\phi_0\int_{\phi_0}^{\infty}\left(\frac{dx}{d\phi}\right)f(\phi_0,\phi)d\phi.$$

For our simple system the conductivity σ_{xx} may be then written, from Pippard,[13]

$$\sigma_{xx}=(4/\pi)(ne^2/\hbar k_0)X,$$

where k_0 is the radius of the Fermi surface.

We will consider scattering with a relaxation time τ by writing $f=\exp[-(\phi-\phi_0)/\omega\tau]$, while at junctions f will also reflect the probabilities P of transmission, a $Q(=1-P)$ of reflection. For this orbit system $dx/d\phi=\frac{1}{2}a\sin\phi$, where a is the diameter of a circular orbit and also the separation of the centers of adjacent circular orbits. Thus,

$$X=\tfrac{1}{4}a\int_0^{\pi}\sin\phi_0 d\phi_0\int_{\phi_0}^{\infty}\sin\phi\, f(\phi_0,\phi)d\phi.$$

Consider electrons created at ϕ_0 on the arc AB of Fig. 10. They travel clockwise on the arc until they reach the junction B, where a fraction P switches to the arc BC while a fraction Q continues on the arc BA. ϕ_0' and ϕ_0'' are defined as the points reached by electrons which have moved through an angle of π from ϕ_0. We can thus split up our integral into the form

$$X=\tfrac{1}{4}a\int_0^{\pi}\sin\phi_0 d\phi_0\Big[P\int_{\phi_0}^{\phi_0'}\sin\phi\, e^{-(\phi-\phi_0)/\omega\tau}d\phi$$
$$+Q\int_{\phi_0}^{\phi_0''}\sin\phi\, e^{-(\phi-\phi_0)/\omega\tau}d\phi+Pe^{-\pi/\omega\tau}\int_{\phi_0'}^{\infty}\sin\phi$$
$$\times f(\phi_0',\phi)d\phi+Qe^{-\pi/\omega\tau}\int_{\phi_0''}^{\infty}\sin\phi\, f(\phi_0'',\phi)d\phi\Big].$$

Bearing in mind the symmetry of the orbits, the last two terms may be identified as

$$Pe^{-\pi/\omega\tau}X-Qe^{-\pi/\omega\tau}X,$$

since by symmetry X is the mean terminal point, relative to the center 0 of the arc BC to which the electron migrates by breakdown, while $-X$ is the mean terminal point of the other half BA of the original orbit. For our simple network, the first two terms may readily be integrated, so that we eventually obtain

$$X=\frac{Pa}{1+1/\omega^2\tau^2}+\frac{Qa}{2\omega\tau}\frac{[1+e^{-\pi/\omega\tau}]}{1+1/\omega^2\tau^2}+(P-Q)Xe^{-\pi/\omega\tau},$$

which may be solved to give

$$X=\frac{ae^{\pi/\omega\tau}}{(1+1/\omega^2\tau^2)}\frac{[P+Q(1+e^{-\pi/\omega\tau})/2\omega\tau]}{[(e^{\pi/\omega\tau}-1)+2Q]},$$

and further simplified if $\omega\tau\gg1$ to

$$X=a(P+Q/\omega\tau)/(2Q+\pi/\omega\tau).$$

Finally, if we may write $Q\gg\pi/2\omega\tau$, i.e., $\omega_0\tau\gg\frac{1}{2}\pi$, then

$$X=\frac{aP}{2Q}+\frac{a}{2\omega\tau},\quad\text{so that}\quad\sigma=-\frac{4}{\pi}\frac{ne^2}{\hbar k_0}X=\frac{B}{H}\left[\frac{P}{2Q}+\frac{1}{2\omega\tau}\right],$$

where B is a constant. This result for X differs from the result obtained in the absence of scattering only by the addition of the term $a/2\omega\tau$.

For the terms σ_{yy} and σ_{xy}, we need merely note that the effective paths L_{yy} and L_{xy} are unchanged by breakdown, so that $\sigma_{yy}\sim1/\omega^2\tau$ while the equal number of electrons and holes implies $\sigma_{xy}=0$ to first order in $1/H$.

APPENDIX B

In this Appendix we will examine the behavior of σ_{xy} for a linear chain of orbits which are not compensated in the absence of breakdown. We will consider the simple system shown in Fig. 10(b) which consists of a network of circular electron orbits with a probability P at each junction of switching to the next orbit and Q of not switching. The mean effective path in the y direction for a semicircular arc may be written

$$Y=\frac{1}{2}\int_0^\pi\sin\phi_0 d\phi_0\int_{\phi_0}^\infty a\cos\phi\, f(\phi_0,\phi)d\phi.$$

This integral splits up, as in Appendix A, to give

$$Y=\frac{a}{2}\int_0^\pi\sin\phi_0 d\phi_0\left[\int_{\phi_0}^\pi\cos\phi\, e^{-(\phi-\phi_0)/\omega\tau}d\phi+P\int_0^{\phi_0'}\cos\phi\, e^{-(\phi-\phi_0)/\omega\tau}d\phi\right.$$
$$\left.+Q\int_\pi^{\phi_0''}\cos\phi\, e^{-(\phi-\phi_0)/\omega\tau}d\phi+Pe^{-\pi/\omega\tau}\int_{\phi_0'}^\infty\cos\phi\, f(\phi_0,'\phi)d\phi+Qe^{-\pi/\omega\tau}\int_{\phi_0''}^\infty\cos\phi\, f(\phi_0,''\phi)d\phi\right].$$

The last two terms may be identified as $Pe^{-\pi/\omega\tau}Y-Qe^{-\pi/\omega\tau}Y$. Evaluating the other terms for our simple example with semicircular arcs, we obtain

$$Y=(P-Q)Ye^{-\pi/\omega\tau}+\frac{a(1-e^{-\pi/\omega\tau})}{\omega\tau(1+1/\omega^2\tau^2)^2}-\frac{\pi ae^{-\pi/\omega\tau}(1+Q-P)}{4(1+1/\omega^2\tau^2)}.$$

Assuming $\omega\tau\gg1$ and $P=1-Q$, then

$$Y=\frac{a/\omega\tau-\pi aQ/2(e^{\pi/\omega\tau}-1)}{1+2Q/(e^{\pi/\omega\tau}-1)}\approx\frac{-\frac{1}{2}aQ\omega\tau}{1+2Q\omega\tau/\pi}+O\left(\frac{1}{\omega\tau}\right).$$

At low fields (but still $\omega\tau\gg1$), $Q\omega\tau>1$, so that $Y=-\frac{1}{4}\pi a$. At high fields, $Q\approx H_0/H$ so that $Y=-a\omega_0\tau/2(1+2\omega_0\tau/\pi)=-\frac{1}{4}\pi a$ if $\omega_0\tau\gg1$. As in Appendix A, we may write $\sigma_{xy}=(4ne^2/\pi\hbar k_0)Y$, so that $\sigma_{xy}=-ne$ for all fields. Thus, in this example breakdown from closed to open orbits does not change σ_{xy} as long as $\omega_0\tau\gg1$. We will assume that this result is true for the more complicated examples appropriate to thallium, which are not so readily calculated. If the network is part of a Fermi surface for which $\sigma_{xy}=0$ before breakdown, then since σ_{xy} is not altered by breakdown, it is zero for all fields.

It is to be expected that this result will be generally true for a linear system of orbits which become coupled by breakdown since at high fields an electron has a finite probability $Q(\approx H_0/H)$ of being switched at each junction from the open orbit to a closed orbit. As long as $\tau\gg1/\omega_0$, an electron which was "created" on the top half of the circle network is as likely to be on the bottom half as the top when it is finally scattered. Thus, the mean terminal point in the y direction is the same as in the uncoupled case and Y is unchanged by breakdown.